Adv. Polar Upper Atmos. Res., **18**, 96–104, 2004

Research note

Auroral O^+ 732/733 nm emission and its relation to ion upflow

Naoko Koizumi[1*], Shoichi Okano[1], Takeshi Sakanoi[1], Makoto Taguchi[2] and Takehiko Aso[2]

[1] *Planetary Plasma and Atmospheric Research Center, Tohoku University, Sendai 980-8578*
[2] *National Institute of Polar Research, Kaga 1-chome, Itabashi-ku, Tokyo 173-8515*
[*] *now at NS Solutions Corporation*

(Received March 3, 2004; Accepted June 10, 2004)

Abstract: Observations of auroral oxygen ion emission at 732/733 nm were made at the Aurora station in Longyearbyen (78.2°N, 16.3°E; $\lambda_m = 74.9°$) using an all-sky spectrograph (ASG) during the winter season of 2000/2001. A statistical analysis showed that the highest occurrence of oxygen ion auroras at Longyearbyen was seen in the dayside of the 09–12 MLT region; the intensities of these auroras were also larger than those on the night side. To study the mechanism of ion upflow in the polar ionosphere, ASG data obtained on December 7, 2000, was analyzed together with simultaneous ionospheric data obtained by EISCAT Svalbard radar (ESR). Enhancements of electron temperature and ion upward velocity were associated with an increase in the auroral OII intensity at the magnetic zenith. This result suggests that an ambipolar electric field associated with electron temperature enhancement caused by soft electron precipitation may be involved in the mechanisms that drive ionospheric ions upward.

key words: aurora, oxygen ion, ion upflow, ESR

1. Introduction

Spectral emission lines at wavelengths of 732/733 nm were first observed by Omholt (1957) and Dufay and Moreau (1957) in low latitude aurora; later, Wallace (1959) identified the spectral origin of these emission lines as oxygen ions. Oxygen ions in aurora are produced by the direct electron impact and ionization of oxygen atoms, 18% of which are excited to a ^{2}P excited state (*cf.* Rees *et al*., 1982) and undergo a transition from ^{2}P to ^{2}D, corresponding to the emission at 732/733 nm.

$$O + e \rightarrow O^+(^2P) + 2e, \quad (1)$$
$$O^+(^2P) \rightarrow O^+(^2D) + h\nu\,(732/733\ \text{nm}). \quad (2)$$

The ^{2}P and ^{2}D states of the oxygen ions are doublets and the wavelengths of the spectral lines emitted by the reaction (2) are 731.892 nm, 731.999 nm, 732.967 nm, and 733.073 nm, according to the Atomic Spectra Database Line Data published by the National Institute of Standards. The ^{2}P state of an oxygen ion has a lifetime of about 5 s; therefore,

quenching dominates at altitudes of lower than 200 km. The OII 732/733 nm emission is effectively produced by soft electron precipitation because a cross section for reaction (1) peaks at about 100 eV. The intensity of auroral OII 732/733 nm emissions is generally low and is liable to be contaminated by the nearby N_2 first positive band. This characteristic of auroral OII 732/733 nm emissions makes observations difficult, and an instrument with a high wavelength resolution and a high sensitivity in this wavelength region is required. Smith *et al*. (1982) observed the OII 732/733 nm aurora using a Fabry-Perot interferometer and a meridian scanning photometer at Longyearbyen in 1982. However, no systematic observations of auroral OII 732/733 nm emissions, which are needed to describe its occurrence characteristics, have been reported so far. Since the motion of ions in the polar ionosphere is governed by the electric field, auroral OII emissions can be regarded as a visible tracer for ion motion. The upflow of heavy ions is frequently seen in the polar ionosphere. However, no direct comparison between ion upflow and auroral OII emissions has been previously reported.

To clarify the occurrence characteristics of the OII aurora, systematic observations were made at the Aurora station in Longyearbyen (78.2°N, 16.3°E; $\lambda_m = 74.9°$) using an all-sky spectrograph (ASG) in the winter season of 2000/2001. Furthermore, to study the mechanism of ion upflow in the polar ionosphere, ASG data on December 7, 2000, was analyzed together with simultaneous ionospheric data obtained by EISCAT Svalbard radar (ESR).

2. Observations

2.1. Instrument

The ASG used in the present study was developed at the National Institute of Polar Research, Japan, and installed at the Aurora station in March 2000. Details of the ASG and its calibration have been previously reported by Taguchi *et al*. (2002). The ASG was initially constructed as a monochromatic all-sky imager (ASI) that employed interference filters to select auroral spectral lines. Operation of the ASI was initiated at Syowa Station in Antarctica in 1998. The ASI was brought back to Japan in 1999 and modified to the ASG by replacing the interference filter with a grism as a dispersive element. The optical layout of the ASG is shown in Fig. 1. The optical system is composed of a fast fish-eye lens ($f = 6$ mm, F1.4), a collimator lens system, a grism with a groove frequency of 600 g/mm, and an imaging lens system. A slit with a width of 42 μm and a length of 20 mm is located at the focal plane of the fish-eye lens. The slit defines a field of view of 0.38 degrees by 180 degrees. A back-thinned bare CCD (512 by 512 pixels) placed at a focal plane of the imaging lens can take images in a form such that the zenith angle and wavelength are aligned along the rows and lines of the CCD, respectively. The CCD is cooled to a temperature lower than -40°C using a three-stage Peltier cooler to minimize dark noise. The pixel size of 24 μm matches the monochromatic images produced by the slit's width. Along the geomagnetic meridian, the CCD resolves a 180 degree field of view into approximately 500 pixels, making the spatial resolution along the meridian about 0.36 degrees. Wavelength coverage is set to 447.1–765.7 nm. Wavelength resolution at 732/733 nm is approximately 2 nm, although this parameter varies slightly depending on the direction of the line of sight. A sensitivity calibration of the ASG was performed at the National Institute of Polar Research

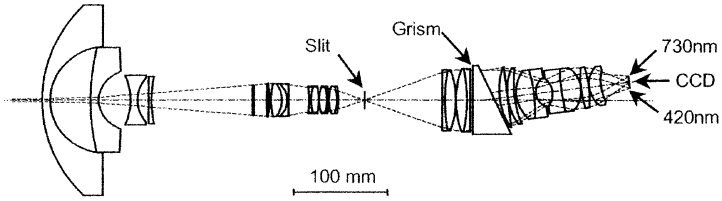

Fig. 1. ASG optics. The optical paths are projected on a plane that includes the optical axes of the fore optics and the focusing optics. The meridional plane is perpendicular to this plane.

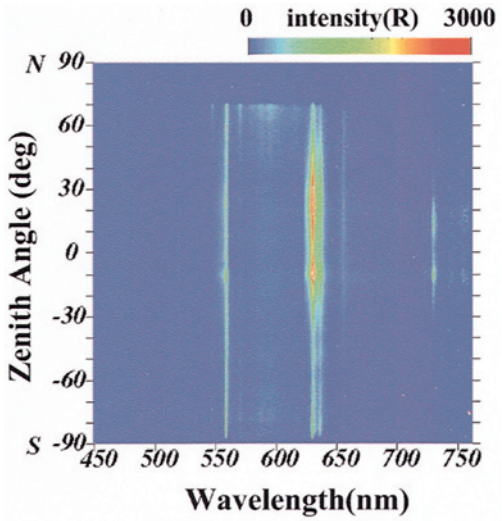

Fig. 2. Spectral image obtained by the ASG at 0756 UT on December 8, 2000. Auroral oxygen green and red lines cover almost the whole sky. The OII emission can be seen around the zenith. The northernmost field of view was blocked by a neighboring building.

using a 2-m integrating sphere as a light source in March 2000. The sensitivity at 560 nm and at zenith was measured to be 0.011 cts/R/s/pixel.

The ASG was installed at the Aurora station in Longyearbyen in March 2000. Routine observations were started in October 2000. Observations were made with an exposure time of 15 s every 3 min. Figure 2 shows an example of a spectral image taken at 0756 UT on December 8, 2000.

2.2. Occurrence and intensity of the OII auroras

The dependence of the occurrence probability and the intensity of the OII auroras on the MLT was studied using data obtained on 21 clear days during the period from October 31, 2000, through to January 20, 2001. Data obtained on days with cloudy sky conditions were excluded from this data set. The total number of spectral images was 3157. To avoid contamination from city lights and twilight, only data within the zenith angles of 60S to 60N were analyzed. With this field of view, the coverage in geomagnetic latitude was $\lambda_m =$

71.3° to $\lambda_m = 78.5°$, assuming that the emission height of the OII auroras was 250 km. Since a multiplet of the OII (^2P–^2D) transition cannot be resolved with the ASG, signals over 7 pixels that corresponded to 4.4 nm centered around 732.5 nm were summed and the background signals within this pixel bin were subtracted from the summed signal to obtain the integrated brightness. This integrated brightness is hereafter referred to as the intensity of the OII aurora. In determining the intensities of the OII emissions, the existence of the nearby N_2 first positive and OH bands was taken into account for each spectral image. The detection threshold for the OII emissions was 30 R. The peak intensity of the OII emissions in each spectral image was taken as the intensity for that time. Therefore, the dependence of the OII aurora on the zenith angle could not be evaluated. To evaluate the magnetic local time dependence of the occurrence probability and the intensity of the OII auroras, the magnetic local time was divided into eight 3-hour sectors and the intensity was classified as less than 200 R, 200–300 R, 300–400 R, 400–500 R, 500–600 R, 600–700 R, or greater than 700 R. Figure 3 shows the occurrence probability of OII auroras at Longyearbyen. From this result, the following points are of interest:

1800–0900 MLT: The occurrence frequency of the OII auroras was 15–20%, and most of the auroras had an intensity of less than 200 R.

0900–1200 MLT: The occurrence probability of the OII auroras was more than 90%. Among the observed auroras, 26%, 58%, and 10% had an intensity of less than 200 R, 200–500 R, and greater than 500 R, respectively.

1200–1500 MLT: The occurrence probability of OII auroras with an intensity of less than 200 R was 37%, while that of auroras with an intensity of greater than 200 R was 29%.

1500–1800 MLT: The occurrence probability of OII auroras with an intensity of less than 200 R was 35%, while that of auroras with an intensity of greater than 200 R was 9%.

These results indicate that most of the OII auroras observed at Longyearbyen appeared mainly in the dayside and that the intensities of the auroras appearing in the dayside were greater than those appearing in the night side. However, it should be noted that the data used in the statistical analysis covered a limited range in geomagnetic latitude and the nightside aurora oval was not fully covered by our observations.

2.3. Simultaneous observation with ESR

During the observation period reported in this paper, the ASG and the 42-m antenna of the ESR were simultaneously operated on December 7, 2000, and the data obtained by both the ASG and the ESR were analyzed for relationships between the OII auroras and ionospheric conditions. Since the field of view of the 42-m antenna of the ESR was directed toward magnetic zenith, the intensities of the OII emissions at the magnetic zenith were compared with the ESR data. Figure 4 shows a keogram of the OII auroras (upper panel) and the time variation of the OII aurora intensity (lower panel) at magnetic zenith (zenith angle −7.7 degrees) on December 7, 2000. Before the sky became cloudy around 0850 UT, intensifications in the OII emissions were seen at around 0513 UT, 0630 UT, and 0745 UT. On the other hand, Fig. 5 shows, from the upper panel to the bottom, the electron density, electron temperature, ion temperature, and ion velocity obtained by the ESR obtained for the same time period shown in Fig. 4. Since the sky became cloudy after 0850 UT, the ASG and ESR data obtained during the time period of 0200–0850 UT were compared. As shown in Fig. 5, increases in the electron density extending to an altitude of 600 km were seen at

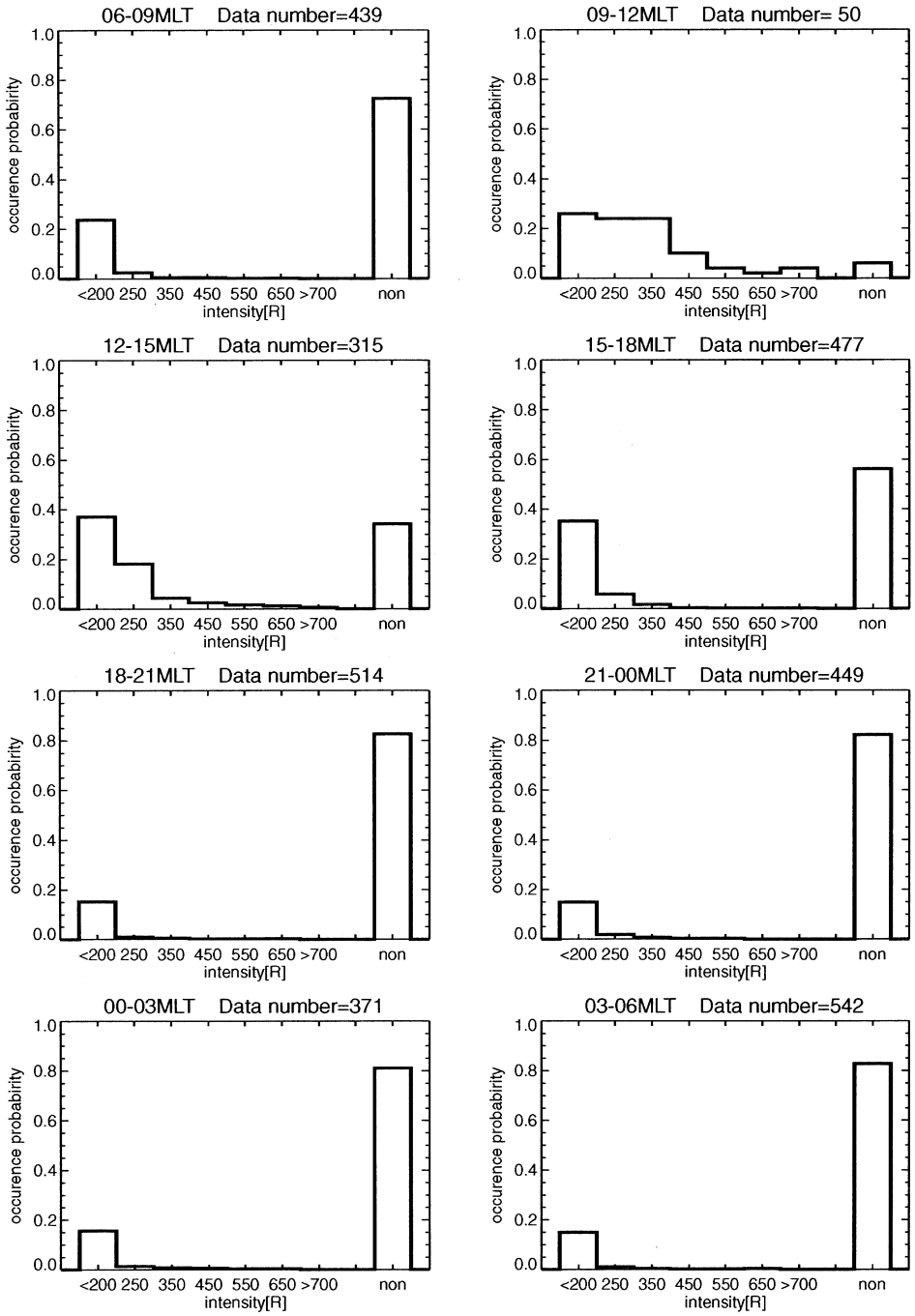

Fig. 3. Occurrence probability of OII auroras sorted according to 3-hour magnetic local time sectors and emission intensities.

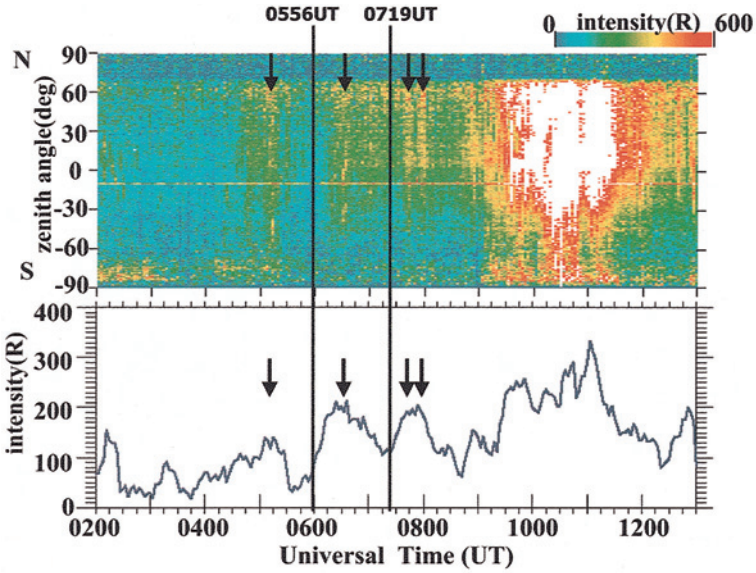

Fig. 4. A keogram (upper panel) and the time variation of the emission intensity at the magnetic zenith (lower panel) of OII aurora on December 7, 2000. Intensifications of the OII auroras are indicated by the arrows. The start and end time points for the correlation analysis with the ESR data are shown by the vertical lines.

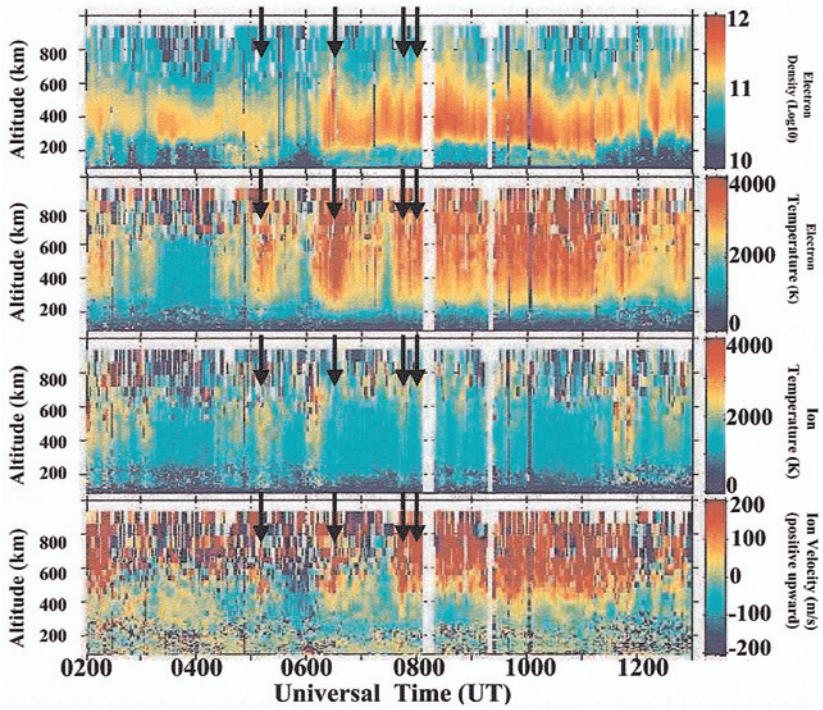

Fig. 5. Ionospheric parameters obtained by the 42-m antenna of the ESR on December 7, 2000. OII intensifications are indicated by the arrows.

around 0630 UT, 0745 UT and after 0800 UT. Increases in the electron temperature were seen above 250 km at around 0510 UT, 0630 UT, and 0745 UT. On the other hand, the ion temperature did not change, except for slight increases at around 0510 UT and 0610 UT. A slight upward ion velocity above 450 km was seen at around 0510 UT, and a more pronounced upward ion velocity was seen at around 0630 UT and after 0750 UT. A correlation analysis between the ionospheric parameters obtained by the ESR and the OII emission intensity at the magnetic zenith obtained by the ASG was performed in the following manner. First, the ionospheric parameters were averaged for 50-km altitude ranges and a time series of each ionospheric parameter for the 50-km altitude bin was made. Then, the correlation between each ionospheric parameter and the OII emission intensity was calculated. Data obtained between 0556 UT and 0719 UT were compared because the most pronounced enhancement of the OII aurora was seen at around 0630 UT. One point that must be taken into account in this analysis is that the time resolutions of the ASG and ESR observations were not identical. The ASG observations were made every 3 min with a 15-s exposure, while the integration time of the ESR observations was 128 s. To ensure a completely simultaneous comparison, only ASG data whose 15-s exposure overlapped with the 128-s integration time of the ESR data were employed in the comparison. Figure 6 shows the correlation coefficients calculated between the intensity of the OII aurora at the magnetic

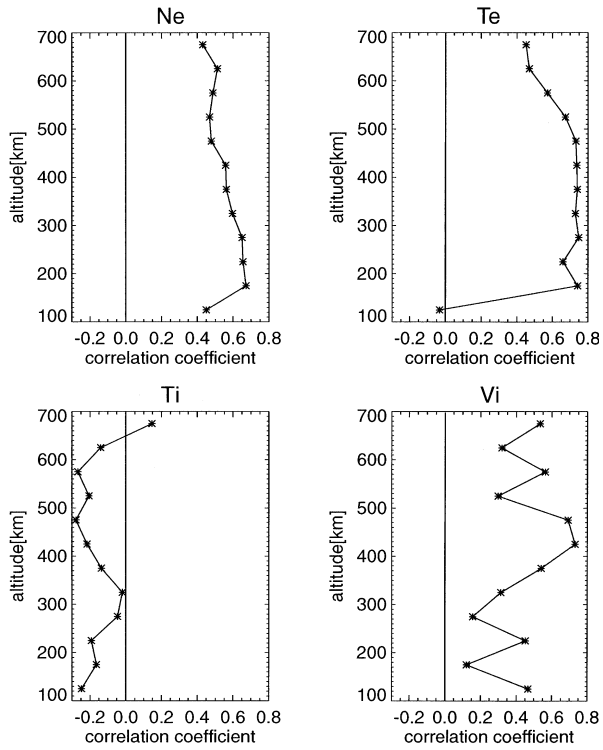

Fig. 6. Correlation coefficients between OII intensity at the magnetic zenith and ionospheric parameters obtained by ESR. Ionospheric parameters are averaged for 50 km altitude ranges.

zenith and each ionospheric parameter averaged for 50-km altitude ranges. As seen in Fig. 6, correlation coefficients of greater than 0.7 were obtained for the electron temperature in the 250–500 km range and for the ion velocity in the 400–500 km range. On the other hand, no correlations between aurora intensity and ion temperature were observed. These results indicate that the electron temperature increased in association with the OII intensity enhancement in the upper *F* region, where the OII emission occurred, and that an increase in the upward ion velocity took place at altitudes 200–300 km higher than the emission height of the OII.

3. Discussion

The statistical analysis of the occurrence probability of the OII aurora reported in the previous section showed that the OII auroras mainly appeared in the dayside and that the intensity of the auroras appearing in the dayside was greater than that of auroras appearing in the night side. The precipitation of soft electrons is known to exist in the dayside cusp region. The Aurora observatory at Longyearbyen is located just under the cusp region in the dayside. In addition, OII auroras are effectively excited by soft electron precipitation. Therefore, our results strongly suggest that the dayside OII auroras observed at Longyearbyen were excited by soft electron precipitation in the cusp region. In addition to the dayside/nightside asymmetry in occurrence probability and intensity observed at Longyearbyen, another asymmetry around magnetic local noon was observed. As seen in Fig. 3, the occurrence probability and the intensity of the auroras were both larger before 12 MLT. This observation may be explained by the results obtained by Liou *et al*. (2001) from the UVI onboard the Polar satellite. In Plate 4 and Plate 5 of the report by Liou *et al*. (2001), the average energy and number flux of the precipitating electrons are shown, respectively. These results show that the average energy was lower and the average number flux was larger for 09–12 MLT, compared with the averages for 12–15 MLT. This means that the soft electron precipitation, which produces the OII 732/733 nm emissions, was more intense before magnetic local noon; our results agree with the Polar UVI observations.

Simultaneous ASG and ESR observations of the OII auroras showed that an enhancement in OII emission intensity was associated with an increase in electron density and electron temperature in an altitude range above 200 km, where OII emissions are thought to occur. An increase in the upward ion velocity was also associated with the OII intensity enhancement. However, the increase in the upward ion velocity was seen at altitudes above 400 km, which is at least 200 km higher than the altitude above which the increases in electron density and electron temperature were observed. One possible mechanism for the upward movement of ions associated with the OII intensity enhancement is proposed below.

As stated previously, OII emissions are effectively excited by the precipitation of soft electrons. The simultaneous enhancement of both OII intensity and electron density and electron temperature suggests that soft electron precipitation occurred at around 0630 UT. An increase in the electron temperature in the *F* region and above results in an increase in the electron scale height; thus, electron heating creates an ambipolar electric field that in turn forces ions upward. However, the collisions of ions with the ambient particles that dominate the lower altitudes prevents the upward motion of ions. On the other hand, the higher the altitude, the fewer the number of collisions that occur, enabling the ions to move

upward more easily. Such a scenario for ion upflow in the *F* region and topside was modeled by Su *et al*. (1999), and ion upflows associated with enhanced electron temperature were observed, without simultaneous observations of OII emissions, by Ogawa *et al*. (2000).

4. Summary

Auroral oxygen ion emissions at 732/733 nm were observed at the Aurora station in Longyearbyen using the ASG during the winter season of 2000/2001. The statistical analysis showed that the highest occurrence of OII auroras (94%) at Longyearbyen was seen in the dayside of the 09–12 MLT region. Overall, 10% of the auroras exhibited an intensity of greater than 500 R in this time sector. On the other hand, in the night side of the 18–09 MLT, the occurrence probability was less than 20% and most of the emissions had an intensity of less than 200 R.

To study the mechanism of ion upflow in the polar ionosphere, ASG data obtained on December 7, 2000, was analyzed together with simultaneous ionospheric data obtained by the ESR. Enhancements in electron temperature and ion upward velocity were associated with an increase in the OII intensity at magnetic zenith. This result suggests that the ambipolar electric field associated with electron temperature enhancement, caused by soft electron precipitation, may be involved in the driving mechanism that leads to ion upflow.

The editor thanks Dr. M. Nakamura and another referee for their help in evaluating this paper.

References

Dufay, M. and Moreau, G. (1957): Spectre de l'aurore du 21 Janvier 1957. Ann. Geophys., **13**, 153–154.

Liou, K., Newell, P.T. and Meng, C.-I. (2001): Seasonal effects on auroral particle acceleration and precipitation. J. Geophys. Res., **106**, 5531–5542.

Ogawa, Y., Fujii, R., Buchert, S.C., Nozawa, S., Watanabe, S. and Van Eyken, A.P. (2000): Simultaneous EISCAT Svalbard and VHF radar observations of ion upflows at different aspect angle. Geophys. Res. Lett., **27**, 81–84.

Omholt, A. (1957): The red and near-infra-red auroral spectrum. J. Atmos. Terr. Phys., **10**, 320–331.

Rees, M.H., Abreu, V.J. and Hays, P.B. (1982): The production efficiency of $O^+(^2P)$ ions by auroral electron impact ionization. J. Geophys. Res., **87**, 3612–3616.

Smith, R.W., Sivjee, G.G., Stewart, R.D., McCormac, F.G. and Deehr, C.S. (1982): Polar cusp ion drift studies through high-resolution interferometry of O^+ 7320-Å emission. J. Geophys. Res., **87**, 4455–4460.

Su, Y.-J., Caton, R.G., Horwitz, J.L. and Richards, P.G. (1999): Systematic modeling of soft-electron precipitation effects on high latitude *F* region and topside ionospheric upflows. J. Geophys. Res., **104**, 153–163.

Taguchi, M., Okano, S., Sakanoi, T., Koizumi, N. and Ejiri, M. (2002): A new meridian imaging spectrograph for the auroral spectroscopy. Adv. Polar Upper Atmos. Res., **16**, 99–110.

Wallace, L. (1959): An analysis of a spectrogram of the aurora of February 11, 1958, in the wavelength range 3710–4420 A. J. Atmos. Terr. Phys., **17**, 46–56.